INTERNATIONAL JOURNAL OF HYDROGEN ENERGY 38 (2013) 5936–5948

Available online at www.sciencedirect.com

SciVerse ScienceDirect

journal homepage: www.elsevier.com/locate/he

# A novel strategy for hydrous-ethanol utilization: Demonstration of a spark-ignition engine fueled with hydrogen-rich fuel from an onboard ethanol/steam reformer

*Gesheng Li*, Zunhua Zhang, Fubing You, Zhixiang Pan, Xintang Zhang, Jian Dong, Xiaohong Gao*

*Key Laboratory of High Performance Ship Technology of Ministry of Education, School of Energy and Power Engineering, Wuhan University of Technology, Wuhan, Hubei 430063, PR China*

ARTICLE INFO

*Article history:*
Received 27 May 2012
Received in revised form
28 February 2013
Accepted 4 March 2013
Available online 29 March 2013

*Keywords:*
Spark ignition engine
Hydrous ethanol
Steam reforming
Onboard reformer
Engine performance
Emission

ABSTRACT

In this paper, an onboard reformer and a dual-fuel (hydrous-ethanol and gasoline) supply system were designed to examine experimentally the reforming performance of hydrous-ethanol for an on-line, operating engine, and a series of optimization and comparison experiments were conducted. The results show that HE75 (75% hydrous-ethanol, i.e., ethanol with 25% water volume content) conversion first increases and later decreases with the temperature and reaches its peak at a temperature of approximately 675 K. The effects of the flow rate and temperature on the product distribution are minimal. Compared to the prototype gasoline-fueled engine, the average decreases of the equivalent specific fuel consumption, $NO_x$ emissions, CO emission and total hydrocarbon emissions for the optimized engine fueled with hydrogen-rich reformates are 6%, 70%, 50% and 80%, respectively. This preliminary experiment suggests that the utilization of hydrous, rather than anhydrous, ethanol in a spark ignition engine by the onboard steam reforming of ethanol may represent a sustainable alternative energy source.



## 1. Introduction

To overcome domestic reliance on expensive and depleting foreign oil, meet the mandatory greenhouse gas (GHG) emissions reduction thresholds, and enhance agriculture and rural economies, national programs around the world are focused on the development, conservation and efficient use of renewable energy. The recent developments in cellulosic conversion technology are renewing interest in bio-ethanol as a practical gasoline alternative candidate for internal combustion (IC) engines [1,2]. Using lignocellulosic biomass, rather than agricultural food feedstocks, to produce ethanol is beneficial to national food grain security because it will not result in a competition between grain supplies and prices [3]. As such, ethanol has been used in IC engines extensively [4,5].

Because of limited intersolubility with gasoline, ethanol is usually used as a gasoline extender (oxygenated fuels) or enhancer (octane booster) at a concentration of 10% or less, except in certain regions, such as Brazil, North America and Sweden [6]. Thus, a limited quantity of ethanol is currently used in IC engines. Moreover, the ethanol applied in IC engines is mainly anhydrous, rather than hydrous, which increases the production cost of anhydrous ethanol in water removal, including distillation and dehydration. It has been

* *Corresponding author*. Tel.: +86 27 87665796; fax: +86 27 86558095.
E-mail address: gsliwh@gmail.com (G. Li).

0360-3199/$ – see front matter 
http://dx.doi.org/10.1016/j.ijhydene.2013.03.008

claimed that the energy required for distillation to reach 80% hydrous-ethanol (HE80, i.e., the aqueous ethanol solution of 20 percent water and 80 percent ethanol in volume) is approximately a quarter of that required to achieve 95.57% [7–9]. It is well-known that HE95.57 is a constant-boiling (azeotropic) mixture; therefore, the use of hydrous ethanol would also avoid dehydration to produce fuel-grade ethanol [8–10]. Therefore, considerable energy can be saved, and emissions can be reduced, if the engine can utilize hydrous ethanol instead of anhydrous ethanol.

Past attempts to burn aqueous fuel have been unsuccessful because of difficulties in initiating combustion for spark ignition (SI) engines and controlling the ignition timing for compression ignition (CI) engines [11]. The modern homogeneous charge compression ignition (HCCI) engine can, however, provide this opportunity because it is inherently fuel flexible and can operate on low-grade fuels (such as ethanol with a high water content), as long as the fuel can be vaporized, sufficiently mixed with air, and heated to the autoignition temperature during the compression stroke [8,9]. Unfortunately, several technical challenges and hurdles remain, such as combustion timing control for transient modes in transportation application, low specific power, high emissions of HC and CO, and difficulty in ignition during a cold start, that have kept HCCI engines from reaching commercial-scale application to date [9].

With the advancement in low-temperature ethanol/steam reforming technology [12–15], there are new ways to use hydrous ethanol. Through this technology, hydrogen-rich mixtures can be derived from the on-board reforming of hydrous-ethanol and can be supplied directly as a potential alternative fuel (i.e., reformed ethanol fuel, RE fuel) to a modified engine (i.e., reformed ethanol engine, RE engine) [15–18]. This low reforming temperature enables heat to be supplied from the engine exhaust. As a consequence, a portion of the energy in the exhaust is recovered [18]. Moreover, because of the unique combustion characteristics of hydrogen [19–27], such as the low ignition energy, high diffusivity and reactivity, and fast burning velocity, the engine fueled with hydrogen-rich mixtures can operate with a higher air-to-fuel ratio or EGR rate. As a result, the engine thermal efficiency can be improved, and $NO_x$ emissions can be reduced [28–36]. In the more recent works, the steam reforming (SR) of ethanol (Eq. (1)) has been reported to apply in IC engines.

$$C_2H_5OH + H_2O \rightarrow 2CO + 4H_2 \quad \Delta H^{\circ}_{298} = +256\ \mathrm{kJ/mol} \tag{1}$$

Tartakovsky et al. [37] conducted a numerical study on the energy analysis of ethanol/steam reforming for hybrid electric vehicles using the software Chem-CAD. The result showed that RE fuel could be an excellent fuel for an IC engine combined with the energy storage system of the hybrid vehicle at lower load driving conditions. Ji et al. [38] investigated the effect of syngas addition generated from the SR of ethanol on a gasoline fueled SI engine. In this test, the fixed engine speed (1800 rpm) and manifold absolute pressure (MAP) (61.5 kPa) were used to ensure the relatively high temperature for SR, and these researchers concluded that the emissions of HC and $NO_x$ decreased with the syngas volume fraction.

Additionally, previous research studies investigating hydrogen production via ethanol steam reforming mainly focused on fuel cell applications [36,39–43]. It is important to note that a high water-to-ethanol ratio is favorable for producing hydrogen. Such a ratio will, however, reduce the power density of RE fuel because of the unreformed hydrous-ethanol. Thus, the reforming performance with a low water-to-ethanol ratio is notably significant for the application of hydrous ethanol in SI engines and has not been previously reported.

Since 2006, the Alternative Fuel Research Group of Wuhan University of Technology has been researching hydrous-ethanol reforming engines, including the low-cost hydrogen production technology via low-temperature plasma and catalytic reforming (as well as the combination of the two approaches) with a low water-to-ethanol ratio via a mini fixed-bed reactor [15,16,44], the premixed combustion character of simulated RE fuel [5,18], and the preliminary exploration of the new possibilities for SI engines to utilize hydrous ethanol, by cooperating with Dongfeng Motor Co., Ltd in China [16,17,45]. Nevertheless, the reforming performance under actual and online engine operating conditions and the optimization of the RE engine directly using the practical RE fuel have yet to be reported in detail.

The motivations of the present study are twofold. The first objective is to enhance the understanding of ethanol/steam reforming with a low water-to-ethanol ratio in real-time engine operating conditions and to determine the main composition of the RE fuel and the conversion efficiency of hydrous ethanol, which can provide basic experimental data and a reference for RE engine optimization. The second objective is to optimize the parameters of the RE engine and investigate the feasibility of an RE engine directly fueled with hydrous ethanol via the steam reforming of ethanol.

## 2. Experimental details

### 2.1. *Reforming reactor and catalyst*

An onboard reforming reactor was designed and employed to investigate the effects of the reaction temperature, flow rate and reaction time on ethanol steam reforming during engine operation as shown in Fig. 1. The reformer was a shell structure containing several u-shaped tubular reactors (copper pipes) with a shell cross-section diameter of 185 mm, and the total weight of the reformer after catalyst loading was approximately 25 kg. The prepared hydrous-ethanol was pumped into the reformer, and it later underwent three processes: vaporizing, overheating and reforming. Specifically, the liquid hydrous-ethanol was evaporated into a gaseous state, and subsequently, the gaseous mixtures were overheated by hot exhaust gases from the engine. Next, the ethanol and steam changed into syngas in the presence of the Cu-based catalyst.

Additional baffles were installed inside the reformer to improve mixing and the heat transfer surface area, which can improve both the effect of evaporation and overheating and provide a somewhat uniform reaction bed temperature. The premix chamber of the reformer served two purposes. The first purpose was to connect the copper pipes of the heating section and the reforming section. The catalyst was loaded in the copper pipes to reform the ethanol/steam gaseous

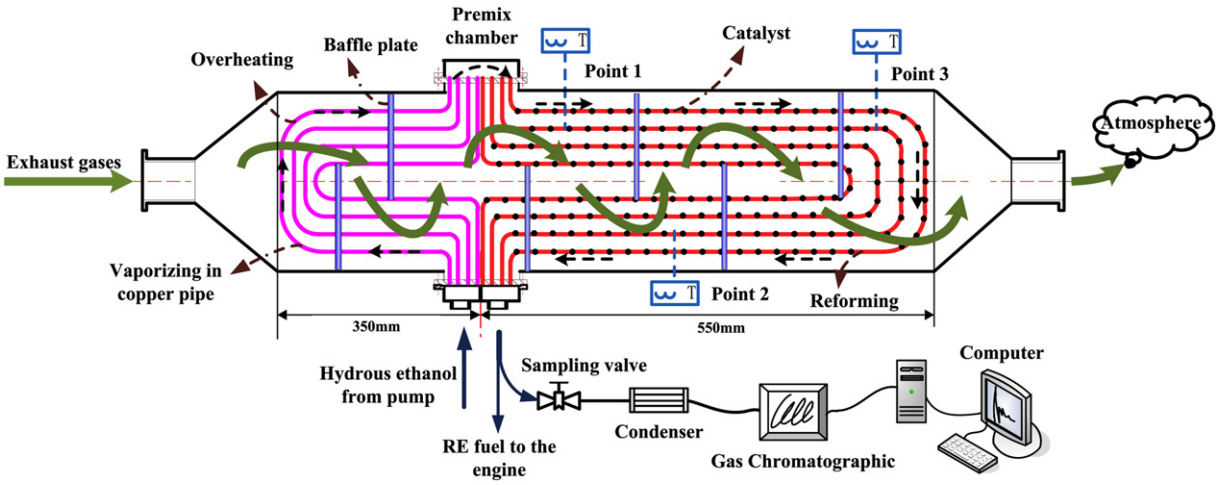


**Fig. 1 – Schematic diagram of the on-board reforming reactor.**

mixtures, and it was necessary to design a chamber to connect the heating section and the reforming section. The second purpose was to mix the gaseous water and ethanol further. More importantly, the difference in the boiling point between water and ethanol could result in a different evaporation rate between the two, and the presence of the chamber could therefore improve the premixing effect of the gaseous mixtures (steam/ethanol) and ensure subsequent homogenous catalytic reactions according to the expected ratio of water to ethanol.

Furthermore, it should be noted that the temperature will decrease with the flowing exhaust gases from the inlet to the outlet of the reformer. That is, a temperature gradient is unavoidable with the exhaust flow. Three different points (front, mid and rear, as shown in Fig. 1), therefore, were set up to record the temperature profile, and the average value of temperature was used in this study.

At the outlet of the ethanol reforming, a separate analysis of the reforming products was performed after condensation via a GC7900 gas chromatograph supplied by Shanghai Techcomp Co., Ltd. The GC was equipped with a Porapak Q packed column (stainless steel) and a molecular sieve column, and the reforming gas was detected using a thermal conductivity detector (TCD). Moreover, the argon was used as the carrier gas in this chromatographic analysis to achieve a high TCD sensitivity for hydrogen, and the flow rate of the carrier gas was maintained at a constant value dependent on the real-time RE fuel consumption of the RE engine. The temperatures at the inlet of the sample and TCD were set as 373 K, while the temperature of the column box was maintained at 303 K for the large peak interval of the chromatograms. In the present measurement, the gas chromatograph (GC) was calibrated by the calibration standard gases supplied by the Wuhan Iron and Steel (Group) Corporation (WISCO). The stability and reproducibility of the temperature control are 0.5% and 2%, respectively, and the minimum sensitivity of the TCD is 10,000 mV ml/mg (for n-hexadecane).

According to the research studies by Maeda and Cavallaro [13,39], this $CuO/ZnO/Al_2O_3$ catalyst exhibited good activity in terms of the hydrogen selectivity with carbon oxides as the main byproducts. In this study, these inexpensive Cu-based catalysts (CB-7: $CuO/ZnO/Al_2O_3$), specially supplied by Sichuan Chemical Co. Ltd, were selected for this experiment. The catalysts were 5 × 5 mm cylinder particles, and they were diluted with similarly sized Pyrex glasses to avoid temperature gradients along the reaction bed.

### 2.2. *Test engine and apparatus*

An EQ6100-1 electronically controlled multi-point injection, water cooling, and SI gasoline engine manufactured by the Commercial Vehicle Engine Plant of Dongfeng Motor Co., Ltd was used in the study. The detailed engine specifications are listed in Table 1. A CW260 eddy-current motoring dynamometer manufactured by Nanfeng Mechanical and Electrical Equipment Co., Ltd was used to measure and control the engine speed and torque. The dynamometer was equipped with a rated torque of 1500 N m/1600–2000 rpm, a maximum speed of 7500 rpm, and absorbed power of 260 kW. The constant torque control precision and the constant speed control accuracy were less than ±0.2% of the full-scale range (FSR) and ±5 rpm, respectively, and the torque measurement sensitivity was less than 0.1%.

The in-cylinder pressure was recorded using a commercial piezoelectric sensor (Kistler 6056A) mounted flush at the cylinder head with the resolution of 10 Pa, and the pressure

**Table 1 – Engine specifications.**

| | |
|---|---|
| Engine type | In-line 6 cylinders, over head valves |
| Bore/stroke | 100 mm/115 mm |
| Total displacement | 5.42 L |
| Compression ratio | 7.0:1 |
| Initial ignition angle | 9–19° crank angle before top dead center |
| Rated power | 99 kW at 3000 ± 100 rpm |
| Peak torque | 352.8 N m at 1200 ± 50 rpm |
| Fuel supply type | Electrical fuel injection (OEM carburetor) |

**Table 2 – Properties of the RE fuel compositions [46].**

| Fuel | Gasoline | Ethanol | Hydrogen | Carbon monoxide | Methane |
|---|---|---|---|---|---|
| Formula | $C_nH_{1.87n}$ | $C_2H_6O$ | $H_2$ | CO | $CH_4$ |
| Molecular weight (g/mol) | ~110 | 46.07 | 2.015 | 28.01 | 16.4 |
| Density at 1 atm and 0 °C (kg/m$^3$) | 720–780 | 780 | 0.09 | 1.25 | 0.72 |
| Lower heating value (MJ/kg) | 44.0 | 26.9 | 120.0 | 10.1 | 50.0 |
| Heat of vaporization at 1 atm and 25 °C (kJ/kg) | 350 | 840 | – | – | – |
| Stoichiometric air/fuel mass ratio; $(A/F)_s$ | 14.6 | 9 | 34.3 | 2.467 | 17.23 |
| Research octane number (RON) | 91–99 | 107 | 130 | – | 120 |

signal was converted into a voltage signal via a Kistler amplifier (Model 5011B), dependent on the range settings. Additionally, a Kistler crank angle encoder (Model 2613B) mounted on the main shaft was used to obtain the corresponding crank angle (CA) position with a resolution of 0.1°CA. The pressure and its corresponding CA signal were acquired via the high speed DL750 Yokogawa data acquisition system, and for each engine operation condition, the pressure data of over 140 successive cycles were averaged to reduce the cycle-to-cycle variability.

An industry standard Horiba chemiluminescence analyzer (Horiba Mexa-1500D) was employed to measure the emission concentrations of HC, $NO_x$, CO, and $CO_2$ and the air-to-fuel ratio (i.e., excess air ratio $\lambda$). The measurement accuracy of the exhaust gas concentration is ±1.0% of the full scale. The emission concentrations reported in the present study were the average results of tests repeated at least three times. For the other standard engine test rig instrumentation, the temperatures were measured using K-type thermocouples with an accuracy of ±1 K. The uncertainty of the mass flow controllers for hydrous ethanol and gasoline was ±1% of the FSR.

### 2.3. *Fuels and fuels supply system*

In the present study, the hydrous ethanol was prepared using anhydrous ethanol (99.95 vol.%) and deionized water at 20 °C and 1 atm, and the volume concentration of the hydrous ethanol was determined by graduated cylinders with 0.5% uncertainty. The water content in the hydrous ethanol, $X_w$, is defined as

$$X_w = \frac{V_w}{V_w + V_e} \times 100\%, \quad (2)$$

where the $V_e$ and $V_w$ are the volumes of ethanol and water, respectively.

Our previous studies showed that RE fuel was composed of $H_2$, CO, $CH_4$, unreformed hydrous-ethanol and other compounds [15,16], and the referred compositions properties of RE fuel are given in Table 2 and compared with gasoline.

There are three reasons for using HE75 (ethanol with a 25% water volume content) to carry out related experimental research. The first reason is the constraint of the freezing point. Pure ethanol has a low freezing temperature of approximately 160 K. However, the freezing temperature

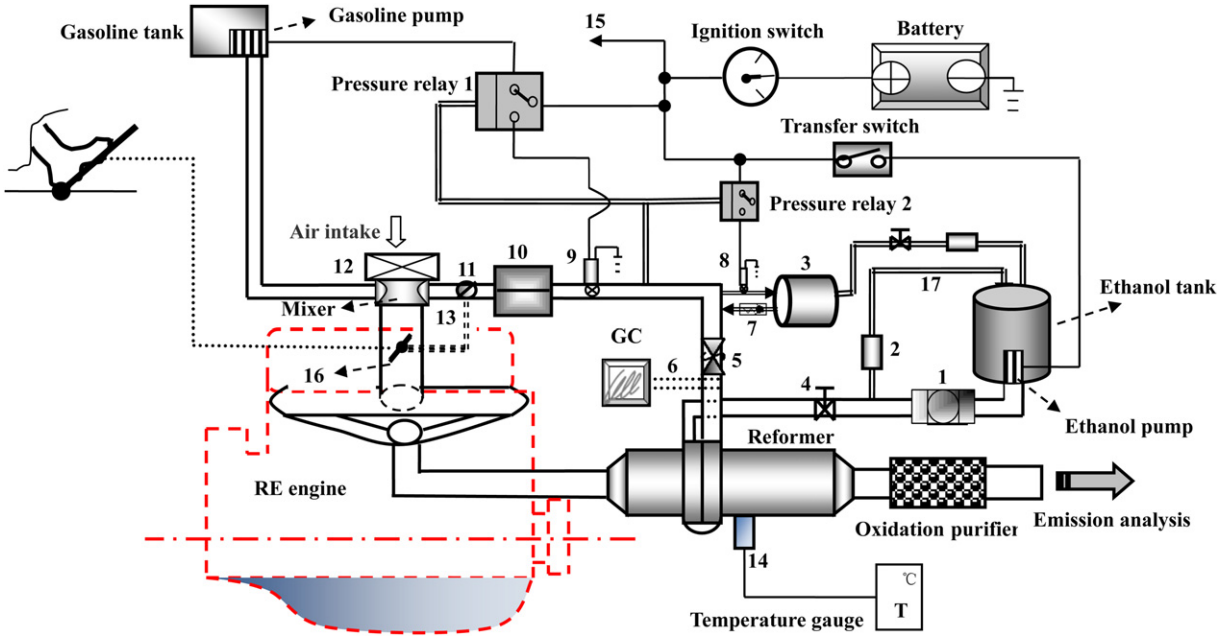


**Fig. 2 – Schematic diagram of the fuel supply system for the RE engine. (1. Ethanol filter; 2. Pressure regulator for liquid ethanol; 3. Pressure stabilizer for the ethanol reformate; 4. Flow control valve for liquid ethanol; 5. Safety valve; 6. Sampling port; 7. One-way valve; 8/9. Shut-off solenoid valve; 10. Pressure stabilizer; 11. Enriching valve; 12. Cooling water chamber; 13. Differential mechanism; 14. Temperature sensor; 15. To ignition system; 16. Throttle; 17. Overflow pipe).**

increases with the increase of the water content in hydrous-ethanol, and when the water content is 40% (HE60), the freezing temperature is approximately 233 K, which is the limit of a liquid fuel [10]. Hence, it is preferable to restrict the water content for a SI engine to less than 40%. The second reason is the lower heating value (LHV). The LHV of pure ethanol is 26.9 MJ/kg (44 MJ/kg for gasoline), and it decreases continuously with increasing water content. Because the enhancement via evaporating, overheating and reforming (endothermic reaction, see Eq. (1)) is limited, using ethanol with high water content is not a viable strategy. The third reason is that the reforming reaction is taken into account. According to the total reaction of ethanol reforming (see Eq. (1)), the molar ratio of water to ethanol is approximately 1:1 (corresponding HE75) for the incomplete reforming of ethanol. Therefore, this particular composition of HE75 is selected provisionally in the present study.

Ethanol/steam reforming is a strongly endothermic reaction; therefore, warming up the reformer is first required. In this study, a special dual fuel supply system is designed for the RE engine cold-start. As shown in Fig. 2, the fuel supply system consists of five sections, i.e., a gasoline supply section, a hydrous-ethanol supply section, a steam reforming section, a RE fuel supply section, and a control section. When starting the RE engine, the transfer switch is set on "gasoline". The RE engine initially operates with gasoline, and the reformer is heated after approximately 5–7 min by the heat exhaust. When the temperature reaches the pre-set value (from the temperature gauge mounted on the reformer), the transfer switch is switched to "hydrous-ethanol". Simultaneously, the hydrous-ethanol pump begins to work, and the subsequent ethanol/steam reforming reaction occurs as mentioned above. If the pressure value of the reformate gas reaches the pre-set value of pressure relay 1, the gasoline pump shuts off, and the RE engine can independently operate with RE fuel. In Fig. 2, a pressure stabilizer is used to regulate and stabilize the pressure of the reformate, which can effectively cope with the change in the operating condition. Additionally, a sampling port is used in the separate chromatographic analysis mentioned above. A cooling water chamber mounted on the mixer is designed to reduce the intake temperatures for higher air density and volumetric efficiency [17]. Fig. 3 shows the modified RE engine test system.

### 2.4. *Experimental procedures*

This experimental study mainly includes three steps, i.e., steam reforming of ethanol, optimization of the RE engine and comparison of the optimized RE engine with the prototype gasoline-fueled engine, and each step is described as follows (the specific test plan and measured parameters are presented in Table 3).

*Step 1*: The reforming characteristics (product distribution, conversion and durability) of HE75 will be investigated. The heat for the reforming was provided by the gasoline-fueled engine exhaust. The temperature was varied via the change of the engine speed and load, and the average temperature from the three different test points was used in the study. This step can provide the basic data for the analysis of the subsequent RE engine test.

*Step 2*: After the SI engine was modified, the parameter optimization of the RE engine was required. In this step, the compression ratio (CR), ignition timing, excess air ratio ($\lambda$), and

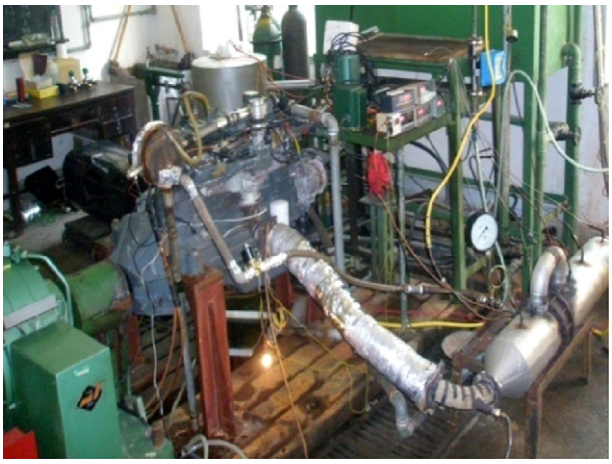

**Fig. 3 – Overview of the test RE engine with an on-board reformer.**

construction of the reformer were optimized at a speed of 2000 rpm and under various loads.

*Step 3*: A comparison of the specific fuel consumption (SFC) and emission of the optimized RE engine with that of the prototype gasoline-fueled engine was carried out at a speed of 2000 rpm and under various loads.

## 3. Results

### 3.1. *Ethanol steam reforming*

#### 3.1.1. *Product distribution*

Fig. 4 shows the reaction temperature dependence of the steam reforming product distribution (vol.% of $H_2$, CO, $CH_4$

**Table 3 – Test plan and measured parameters for the present study.**

| Experiments | Measured parameters | |
|---|---|---|
| | Independent variables | Dependent variables |
| Steam reforming of ethanol | Test temperature, Mass flow rate | Product distribution, HE conversion |
| | Test time, SEM images | Catalyst endurance and activity |
| Optimization of RE engine | Compression ratio, Speed | Specific fuel consumption (SFC), Maximum torque, Emissions (THC, CO, $NO_x$) |
| | Ignition timing | In-cylinder pressure, SFC, Emissions |
| | Excess air ratio, Load | SFC, Emissions |
| | Reformer structure, Load | Brake thermal efficiency, Backpressure |
| Comparison of RE engine with prototype engine | Fuel, Load | SFC, Emissions |

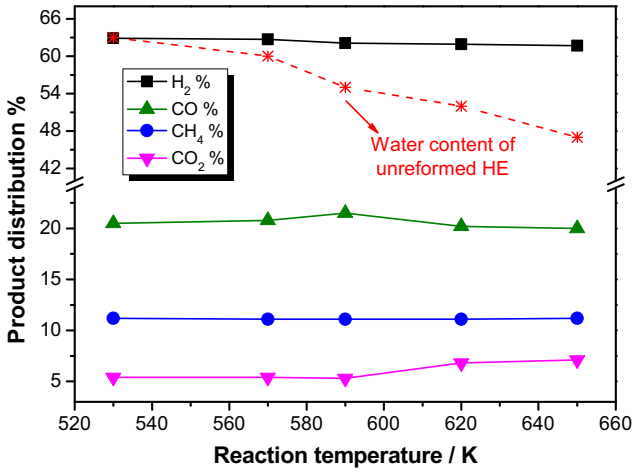


**Fig. 4 – Effect of the reaction temperature on the product distribution of ethanol/steam reforming at a flow rate of 16 g min$^{-1}$.**

and $CO_2$) and the water content of unreformed hydrous-ethanol ($X_w$) at a given hydrous-ethanol flow rate. Based on the reaction in Eq. (1), the equilibrium yield mole ratio of hydrogen-to-carbon monoxide is theoretically two to one. However, the yield of hydrogen shown in the figure is approximately 3 times that of CO. This result suggests that a portion of the CO is involved in other reactions, such as the water gas shift (WGS) reaction and the Boudouard reaction (see Eqs. (3a) and (3b), respectively).

$$CO + H_2O \rightarrow 2CO_2 + 4H_2 \quad \Delta H^{\circ}_{298} = -41.2\ \text{kJ/mol} \tag{3a}$$

$$2CO \rightarrow CO_2 + C \quad \Delta H^{\circ}_{298} = -171.5\ \text{kJ/mol} \tag{3b}$$

In addition, there is small amount of $CH_4$ and $CO_2$, and the $CH_4/CO_2$ mole ratio is approximately 2:1 when the temperature is less than 600 K. The thermodynamic equilibrium analysis indicates that ethanol/steam reforming cannot occur when the reaction temperature is less than 500 K, at which $\Delta G$ (change of the Gibbs function) is greater than zero [43]. This result means that the $CH_4$ and $CO_2$ is obtained mainly from the decomposition reaction of ethanol (see Eq. (4)), which is strongly favored at low temperatures (<473 K) [43].

$$C_2H_5OH \rightarrow 0.5CO_2 + 1.5CH_4 \quad \Delta H^{\circ}_{298} = -74\ \text{kJ/mol} \tag{4}$$

When the temperature is higher than 600 K, the yield of $CO_2$ increases with increasing temperature, while the opposite relationship is observed for CO, which implies that increased temperature can enhance the conversion of the WGS reaction [14]. In fact, this property can be confirmed from the decreasing water content of the unreformed hydrous-ethanol with the temperature in the figure. That is, steam is part of the reforming reaction and promotes the dehydration reaction of the ethanol due to the acid $Al_2O_3$, as shown in Eq. (5):

$$C_2H_5OH \rightarrow C_2H_4 + H_2O \quad \Delta H^{\circ}_{298} = 45\ \text{kJ/mol} \tag{5}$$

With the presence of ethylene, carbon deposition is intensified because of the polymerization reaction (Eq. (6)) and the Boudouard reaction (Eq. (3b)), which results the decreasing activity of the catalyst.

**Table 4 – Average product distribution of hydrous ethanol reforming.**

| Product | $H_2$ | CO | $CH_4$ | $CO_2$ | $C_2H_4$ | $C_2H_6$ | Others |
|---|---|---|---|---|---|---|---|
| Concentration vol.% | 60.1 | 20.5 | 10.8 | 5.4 | 2.0 | 1.1 | 0.1 |

$$C_2H_4 \rightarrow \text{polymers} \rightarrow 2C + 2H_2 \tag{6}$$

Generally, the effect of temperature on the product distribution of ethanol reforming is not significant at temperatures ranging from 530 to 600 K. Additionally, the product distribution is observed to present a notably slight dependence on the flow rate of hydrous ethanol, which is not shown in the figure. As a consequence, the average product concentrations (see Table 4) are used to simplify the analysis of the engine test in this study. This phenomenon is consistent with the report from Maeda et al. [13].

### 3.1.2. *Hydrous ethanol conversion*

The conversion of hydrous ethanol is another important factor in terms of ethanol reforming. In the present study, the hydrous ethanol conversion, $C_{HE}$, is defined as

$$C_{HE} = \frac{\dot{m}_{in} - \dot{m}_{out}}{\dot{m}_{in}} \times 100\%, \tag{7}$$

where $\dot{m}_{in}$ and $\dot{m}_{out}$ are the mass flow rates of hydrous-ethanol in and out of the reformer, respectively.

Fig. 5 shows the effect of the reaction temperature and flow rate on the HE conversion. The conversion first increases and then decreases with the temperature, and the maximum value occurs at a temperature of approximately 675 K, indicating the highest catalyst activity. Fig. 5 also shows that there

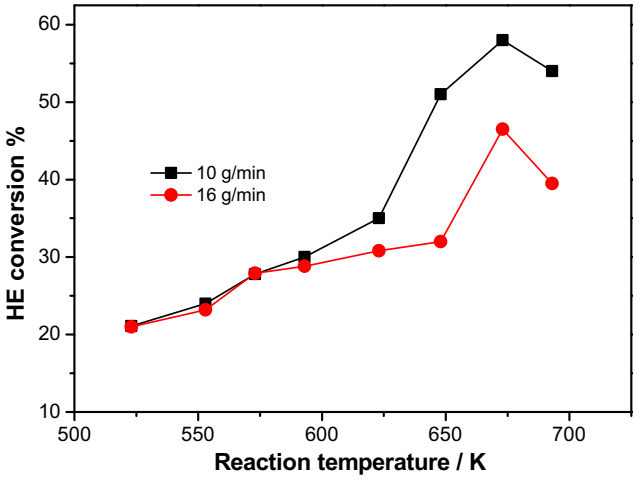


**Fig. 5 – HE conversion at different reaction temperatures and HE flow rates.**

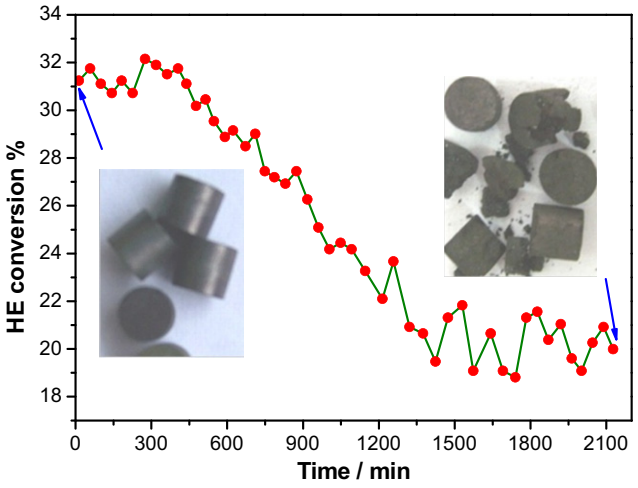


**Fig. 6 – Variation of the HE conversion versus time at a reaction temperature of 620 K.**

is little dependence on the flow rate for the HE conversion when the temperature is less than 600 K. However, the conversion begins to decrease with increasing flow rate when the temperature is greater than 600 K.

#### 3.1.3. *Endurance test*

The durability of the catalyst is an important parameter, and an endurance test (approximately 2200 min) was conducted at a reaction temperature of 620 K, as shown in Fig. 6. The HE conversion first fluctuates approximately 31% when the time is 300 min or less, and the conversion subsequently decreases almost linearly until 1300 min. Finally, the conversion fluctuates approximately 21% with the increase of the test time. The actual pictures of the catalysts before and after the reaction are given in Fig. 6. Pulverization and coking are observed and may be the reason for the decrease of the catalyst activity.

To investigate the metal sintering phenomena, which can largely govern the stability and aging of the catalyst [41], the scanning electron microscope (SEM) images of Cu-based catalysts before and after the reforming reaction at 620 K are shown in Fig. 7. Before the reforming reaction, the active component of the catalyst has an average size of 300 nm and is uniformly distributed on the substrate surface of the catalyst (Fig. 7a and b). After the reforming reaction, most of the active component aggregates and is approximately 600–900 nm (Fig. 7c and d), which illustrates the rapidly reduced activity of Cu-based catalysts. That is, the larger size of the active component reduces the surface area, which reduces the catalytic activity.

### 3.2. *Optimization of the RE engine parameters*

#### 3.2.1. *Dependence on CR*

Although hydrous ethanol has the lower heating value than gasoline, it has a higher octane value (see Table 2); therefore, the power performance of an RE engine can be improved using the elevated compression ratio (CR). In the present study, two different CRs (7.0 and 8.5) were used, and the influence of the CR on the maximum torque and specific fuel consumption (SFC) at different speeds for the RE engine at wide-open throttle are illustrated in Fig. 8. The figure shows that as the

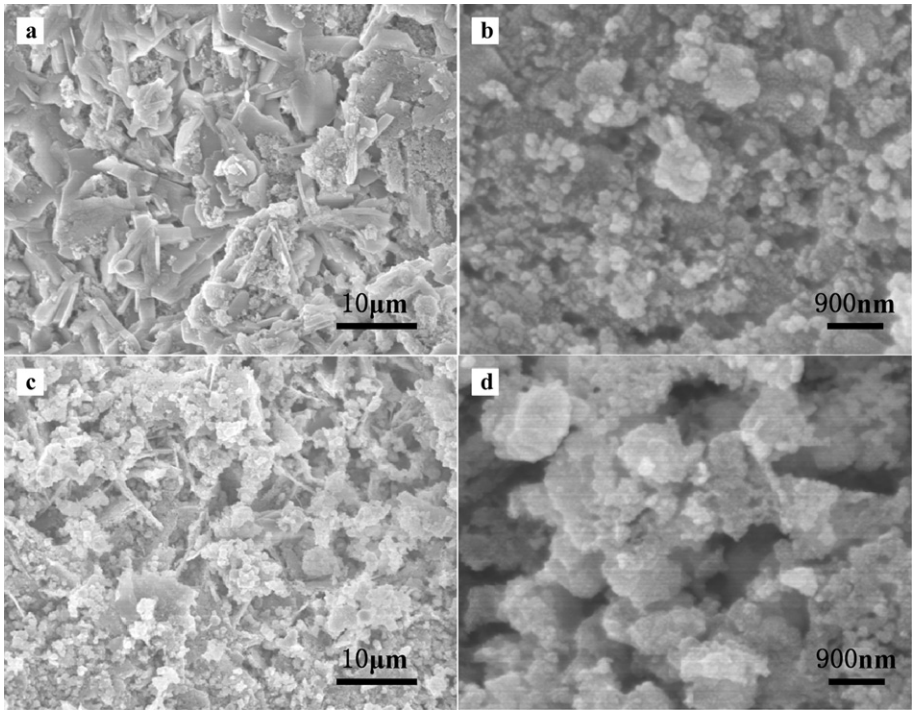


**Fig. 7 – SEM images of the catalysts before and after reaction at 620 K (a and c are the fresh catalysts with magnifications of 20 k and 150 k, respectively; b and d are the reacted catalysts with magnifications of 20 k and 150 k, respectively).**

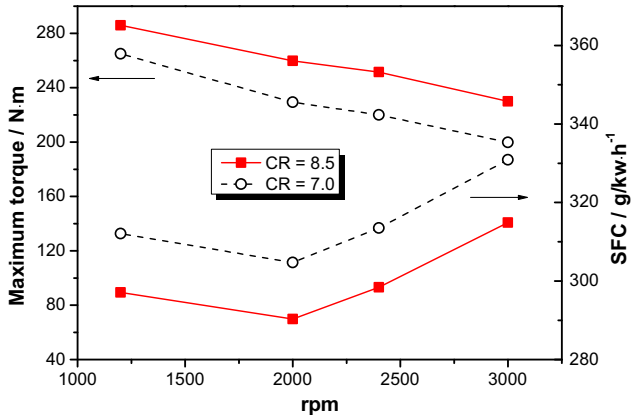


**Fig. 8 – Effects of the compression ratio on the maximum torque and specific fuel consumption (SFC) at different speeds for the RE engine under wide-open throttle.**

engine speed increases, the peak torque decreases. When the CR increases from 7 to 8.5, the peak torque increases by approximately 8% and 15% at the speeds of less than and greater than 2000 rpm, respectively. Additionally, the SFC improves by approximately 6.3%. Moreover, an increase in the CR will result in a slight increase in $NO_x$ emissions. Therefore, the enhancement of the CR can improve the power performance as well as the fuel economy of the engine. Because of limitations of the engine components, a higher CR was not examined in this study.

### 3.2.2. *Dependence on the ignition timing*

The empirical rule for the optimum spark timing is that the maximum cylinder pressure should occur at a CA of 12–15° after the top dead center (TDC) to ensure soft operation and good power performance and to avoid abnormal combustion (called *knock*), i.e., the minimum advance for the best torque [4,46]. Fig. 9 gives the cylinder pressure as a function of the crank angle at different spark timings (9, 16 and 19° before the TDC) for the RE engine. When the angle of ignition advance is

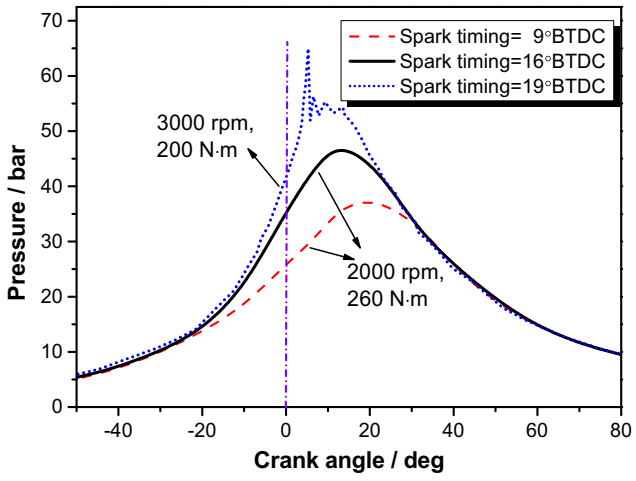


**Fig. 9 – Effect of the ignition timing on the cylinder pressure for the RE engine (BTDC, before top dead center).**

at a CA of 9° before the TDC (i.e., un-optimized prototype gasoline engine), the maximum pressure (37.96 bar) occurs at a CA of approximately 20° after the TDC with the RE engine operating at 2000 rpm and 260 N m. In the case of spark timing at a CA of 16° before the TDC, the maximum pressure occurs at a CA of approximately 14.2° after the TDC, and it is increased by 10.1 bar compared to the un-optimized spark timing (CA of 9° before the TDC). Furthermore, as the angle of ignition advance continues to increase up to a CA of 19° before the TDC, the intense knock is present at the RE engine, which is operating at 3000 rpm and 200 N m, as shown in Fig. 9. As such, a CA of 16° before the TDC is used to optimize the spark timing of the RE engine in the present study.

After the optimization of the spark timing, the SFC and exhaust temperature decreased somewhat. Moreover, although the $NO_x$ and THC emissions increased slightly with the increase in the angle of ignition advance, the emissions levels were still less than those of the prototype engine fueled with gasoline, which will be compared in the subsequent section.

### 3.2.3. *Dependence on lean combustion control*

Lean combustion is a particularly attractive means to reduce emissions and save energy for modern IC engines [33]. The lean-burn operation of an SI engine offers low temperature combustion due to the dilution of the excess air and, consequently, the rapid reduction of $NO_x$ emissions, as well as wall heat loss. In addition, at partial load, the brake thermal efficiency (BTE) can be improved by decreasing the pumping work due to the increased intake manifold absolute pressure (MAP) at a fixed torque. Furthermore, lean combustion can efficiently avoid knock and enhance the BTE via the increased CR mentioned above. In the case of lean combustion, rather than ultra-lean combustion, a sufficient amount of oxygen can oxidize the HC and CO more completely and thereby reduce emissions.

Fig. 10a illustrates the variations of the emissions and SFC versus lambda at 2000 rpm and 180 N m. The figure shows that the emissions and SFC are optimal for lambda ranging from 1.1 to 1.25. For a richer mixture ($\lambda < 1.05$), the CO and total hydrocarbon (THC) emissions and the SFC increase dramatically as lambda decreases. For a leaner mixture ($\lambda > 1.25$), although the $NO_x$ emissions are reduced somewhat as lambda increases, the increase in the SFC and CO and THC emissions are rapid because of incomplete combustion.

Based on Fig. 10a, the control strategy of lambda for an RE engine combined with quantity and quality regulation at a constant speed is given in Fig. 10b. When the RE engine is idle, and the exhaust temperature is low, corresponding a lower HE conversion, a richer mixture is needed. That is, a lower lambda ($\lambda = 1.01–1.03$) is used under idle and lower load conditions. With the increase in the load of the RE engine (0–75%), the throttle opening and exhaust temperature increases, resulting in a higher HE conversion and hydrogen fraction in the RE fuel. During this stage (named target zone), the lean-burn ($\lambda = 1.03–1.37$) can be used, and the lambda increases with the increased load. The largest lambda value can reach 1.37 at a load of approximately 70%. The control in this stage is named "quantity regulation". For a higher load (75–100%), the RE engine is in wide-open throttle operation,

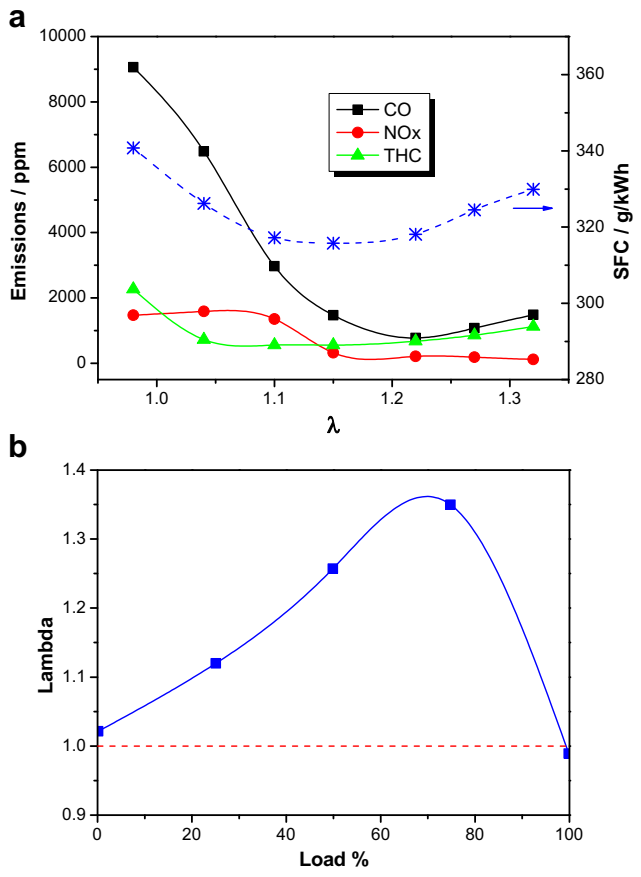


**Fig. 10 – Control strategy of lean-burn for the RE engine (a. effect of the excess air ratio on the SFC and emissions at 2000 rpm and 180 N m; b. control strategy of the lambda combined with quality and quantity regulation at a speed of 2000 rpm).**

and to ensure power output, a particular enhancing valve, shown in Fig. 2, is used to decrease the lambda rapidly to 0.98–1.0. Therefore, the lambda control in this stage can be called "quality regulation". It should be noted that a lower lambda (<0.95) is unreasonable because the higher the load is, the larger the HE conversion is, thereby increasing the CO fraction in RE fuel. If the lambda is insufficient, the CO emission and SFC will increase dramatically, as shown in Fig. 10a.

### 3.2.4. *Dependence on the structure of the reformer*

The flow resistance of the exhaust gas will increase because of the mounting of an on-board reformer after the outlet of the exhaust manifold. On the one hand, high exhaust flow resistance will cause the increase of push work of the piston in the exhaust processes. On the other hand, the exhaust backpressure will increase with the increased flow resistance, resulting in a high residual gas fraction or backflow of exhaust gas into the cylinder. This finding means that a high flow resistance will have a negative influence on the engine brake thermal efficiency (BTE) and the power output, which must be compensated for by increasing fuel consumption. Therefore, the main consideration for improving and optimizing the reformer structure is to reduce the backpressure and maintain good heat transfer as far as possible.

The use of a U-shaped tube instead of a serpentine tube can remarkably improve the heat transfer coefficient. Additionally, Fig. 11 shows the typical improvement in the reformer structure to reduce the flow resistance of exhaust gas (i.e., reduce the exhaust backpressure). Compared to reformer 1 (unimproved), the improved reformer (reformer 2) uses fewer baffles and lets the exhaust gas downstream. That is, this reformer does not allow the exhaust gas through the flange (connecting the heating section and reforming section) in a roundabout way. Fig. 12 shows the exhaust backpressure and brake thermal efficiency as a function of the loads with reformer 1 (unimproved) and reformer 2 (improved). As seen in Fig. 12, the drop of the backpressure is significant after

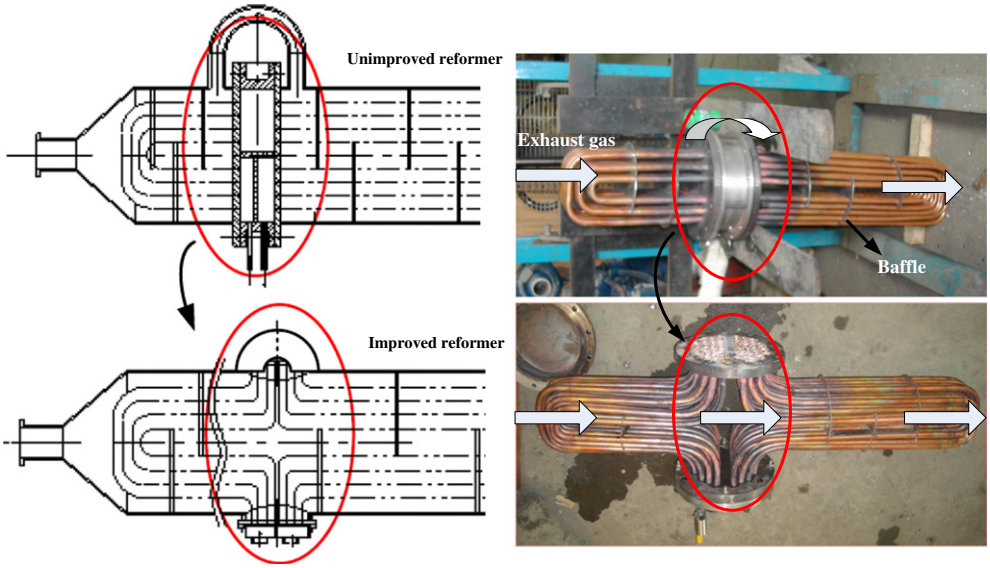


**Fig. 11 – Internal structures of the unimproved (Reformer 1) and unimproved (Reformer 2) reformers.**

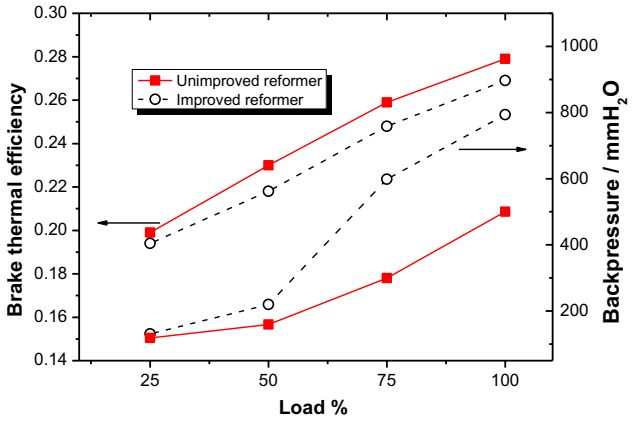


**Fig. 12 – Effect of the reformer structure on the exhaust backpressure and brake thermal efficiency at 2000 rpm with various loads.**

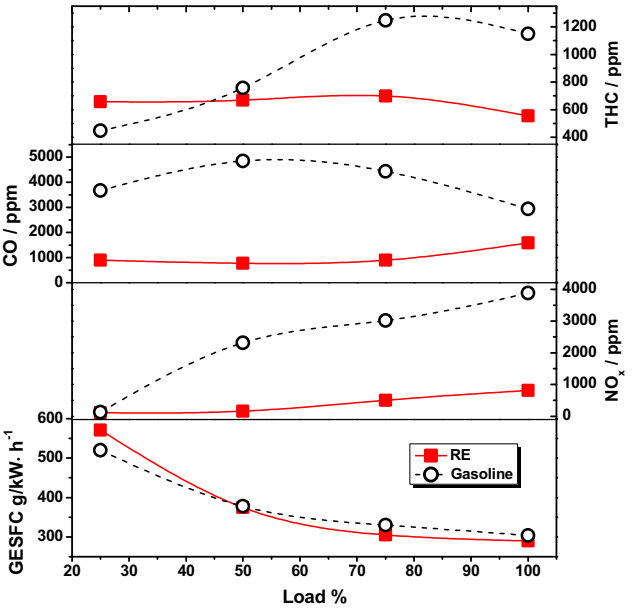


**Fig. 13 – Experimental comparison of the SFC and emissions between the optimized RE engine with the prototype engine fueled with gasoline operating at 2000 rpm and various loads.**

optimization, especially at a high load, which improves the BTE.

### 3.3. *Comparison of the optimized RE engine with the prototype gasoline engine*

To demonstrate the feasibility of the RE engine fueled with RE fuel from on-board ethanol/steam reforming, a comparison experiment of the optimized RE engine with the prototype engine fueled with gasoline is carried out at 2000 rpm. As shown in Fig. 13, the RE engine fueled with HE75 reforming gas is started via gasoline and operates with a CR of 8.5, a spark timing of a CA of 16° before the TDC and a lambda combined with quality and quantity regulation. Conversely, the prototype engine operates with the parameters mentioned in Table 1. To enhance the comparability, the measured value of the specific fuel consumption (SFC) of the RE engine is the equivalent value of hydrous ethanol to gasoline based on the LHV (i.e., gasoline equivalent specific fuel consumption: GESFC). If we assume that the LHVs of the gasoline and HE75 are 44 and 19 MJ/kg, respectively, the consumption of 1 g of HE is equivalent to 0.43 g of gasoline based on the LHV. Therefore, the GESFC can be defined as

$$\mathrm{GESFC} = \frac{\dot{m}_{\mathrm{HE}} \times \dfrac{\mathrm{LHV}_{\mathrm{HE}}}{\mathrm{LHV}_{\mathrm{gasoline}}}}{P_{\mathrm{RE}}} \times 100\%, \tag{8}$$

where $\dot{m}_{\mathrm{HE}}$ is the mass flow of HE per unit time; $\mathrm{LHV}_{\mathrm{HE}}$ and $\mathrm{LHV}_{\mathrm{gasoline}}$ are the LHV of the HE and gasoline, respectively; and $P_{\mathrm{RE}}$ is the power output of the RE engine.

Fig. 13 shows that the GESFC and emissions improve significantly at almost all loads, except for the GESFC and THC emissions at a low load (25%). This is the result of incomplete combustion due to the low exhaust temperature (see Table 5) corresponding to the low HE conversion and hydrogen fraction in the RE fuel (see Fig. 5). In addition, the difference of the CO emission between the prototype and RE engine decreases with increasing load. This phenomenon is mainly caused by the high CO fraction in RE fuel due to the lower lambda strategy at high loads, inducing a high exhaust temperature and HE conversion, which is consistent with Fig. 10.

Although the power performance is found to decrease for the RE engine, the reduction of the maximum torque is approximately 5% compared to the prototype gasoline fueled engine. Additionally, the average decrease in the quantities of GESFC, $NO_x$ emissions, CO emission and THC emissions are approximately 6%, 70%, 50% and 80%, respectively. This finding indicates that the utilization of hydrous ethanol in an SI engine via onboard ethanol/steam reforming is feasible.

## 4. Discussion

This preliminary investigation tried to experimentally demonstrate the feasibility of an SI engine fueled with 75% hydrous-ethanol (HE75) via an onboard reformer. A special onboard reformer and hydrous-ethanol supply system were designed to examine HE75 reforming under engine operation and the performance and emissions of the SI engine fueled with hydrogen-rich mixtures from hydrous-ethanol reforming. Upon comparison with the prototype gasoline-fueled engine, the RE engine, with its increased compression ratio and lean-burn means, presented a promising opportunity to utilize hydrous ethanol instead of anhydrous ethanol, which can substantially reduce the cost in producing fuel-grade ethanol during the distillation and dehydration processes.

As a matter of fact, both ethanol steam reforming and the hydrogen-rich engine are not new concepts, and neither is the utilization of hydrous ethanol in IC engine, which has been applied in HCCI engines. Nevertheless, the hydrogen-rich mixtures via steam reforming (SR) of ethanol used in an SI

**Table 5 – Temperature of the different test points in the reformer at various torque values.**

| Torque (N m) | Test point 1, $T_1$ (K) | Test point 2, $T_2$ (K) | Test point 3, $T_3$ (K) | Equivalent temperature, $T_e = (T_1 + T_2 + T_3)/3$ (K) |
|---|---|---|---|---|
| 65 | 543 | 493 | 393 | 476 |
| 130 | 603 | 553 | 413 | 536 |
| 195 | 653 | 593 | 428 | 558 |
| 260 | 673 | 623 | 453 | 583 |

engine has not been previously investigated. For many years, ethanol/steam reforming has been studied intensively for fuel cell applications. It is well-known that the CO in reformate is intolerable because of its toxicity for proton-exchange membrane fuel cells. The irreversible damage and hindering of the electrochemical reaction for Pt-based electrodes occurs as the concentration of CO becomes greater than 20 ppm [47,48]. To make matters worse, there exists a kinetic limit between high hydrogen selectivity and the WGS reaction used to reduce the CO concentration [41,47]. Consequently, numerous previous research studies on the SR of ethanol have attempted to obtain the maximum hydrogen yield, but a large water-to-ethanol mole ratio (>3 at least) and a high reaction temperature (>650 K) are required.

With respect to the IC engine, CO is a flammable gas and can be used as a fuel. That is, the purification process of ethanol reformate is not essential for IC engine feeding. In addition, a high water-to-ethanol mole ratio reduces the energy density of the fuel, and a high temperature via engine exhaust heat is unrealistic (see Table 5). As a result, the present report, in terms of an SI engine fueled with on-board ethanol reformate, leads to two new research areas and interests, which are quite distinct for full cell applications, i.e., 1) ***RE fuel***, derived from the SR of ethanol at a low temperature and water-to-ethanol ratio condition to obtain a high engine efficiency instead of a large hydrogen yield; and 2) ***RE engine***, fueled with an on-board hydrogen-rich gas, including $H_2$, CO, $CO_2$, and $CH_4$, for the purpose of optimizing engine performance and emissions.

The selection of the catalyst and the design of the reformer are highly vital for the commercial scale application of an RE engine fueled with RE fuel. In the present study, the hydrous-ethanol conversion was high during the initial stage, whereas metal sintering and coking rapidly deactivated the catalyst over time (see Figs. 6 and 7). Moreover, it is crucial to minimize the ethanol dehydration reaction at a low water-to-ethanol ratio and reduce coking (see Eqs. (5) and (6)). Extra effort should be expended on improving the activity, durability and conversion of the catalyst for RE fuel commercial feasibility. Moreover, developing an efficient, compact and portable reformer for RE engines is also underway. It should be noted that the optimization of the water content in the HE for RE engines and the combustion characteristics of RE fuel have yet to be illustrated in detail, and further investigations are therefore still warranted.

Although the RE engine operating under lean-burn conditions produces fewer pollutants (see Figs. 10 and 13), this advantage could be counterbalanced by the reduced efficiency of the 3-way catalyst. Hence, another issue of practical importance is reducing the $NO_x$ emissions of the lean-burn RE engine.

## 5. Conclusions

The present report could suggest a new application for hydrous-ethanol in IC engines, although further investigation is still required. The major conclusions from the study can be summarized as follows:

The HE conversion increased with the temperature, reaching a peak at approximately 675 K. In addition, a downward trend for the conversion with the flow rate was observed at temperatures above 600 K. The product distribution of HE reforming was not sensitive to the feed flow rate. The HE conversion fluctuated approximately 31% when the test time was less than 300 min, and the conversion subsequently decreased almost linearly until 1300 min. Finally, the conversion fluctuated approximately 21% after 1300 min. Pulverization, coking and sintering were observed and were believed to be the major reason for the deactivation phenomena of the catalysts.

When the CR of the RE engine increased from 7 to 8.5, the peak torque increased by approximately 8% and 15% when the speeds were less than and greater than 2000 rpm, respectively. A CA of 16° before the TDC was observed to be the optimum ignition timing for the RE engine at 2000 rpm. Flow resistance due to the onboard reformer was found to have a substantial influence on the RE engine's brake thermal efficiency, especially at high load. The emissions and SFC was optimal for lambda ranging from 1.1 to 1.25 for the RE engine, and a control strategy combined with the "quality and quantity regulation" of lambda at a constant speed was developed to achieve lean-burn.

Compared to the prototype gasoline fueled engine, the optimized RE engine was found to decrease, on average, the quantities of gasoline-equivalent specific fuel consumption, $NO_x$ emissions, CO emission and THC emissions by approximately 6%, 70%, 50% and 80%, respectively. In general, it can be concluded that using hydrous ethanol in an SI engine by an onboard reformer represents a sustainable alternative energy source.

## Acknowledgments

This work was financially supported by the Natural Science Foundation of Hubei Province under Grant 2011CDA058 and by the Program of Introducing Talents of Discipline to Universities under Grant B08031. Assistance with setting up and testing the experimental facilities from the "Alternative Fuel Research Group of WUT" was also important, which is deeply appreciated. Our special thanks are due to Dr. Zhan Hongju for providing useful advice and discussions regarding the steam reforming of ethanol.

## REFERENCES


[1] Balat M, Balat H. Recent trends in global production and utilization of bio-ethanol fuel. Appl Energy 2009;86(11):2273–82.

[2] Farrell AE, Plevin RJ, Turner BT, Jones AD, O'Hare M, Kammen DM. Ethanol can contribute to energy and environmental goals. Science 2006;311(5760):506–8.

[3] Schmer MR, Vogel KP, Mitchell RB, Perrin RK. Net energy of cellulosic ethanol from switchgrass. Proc Natl Acad Sci U S A 2008;105(2):464–9.

[4] Costa RC, Sodré JR. Hydrous ethanol vs. gasoline-ethanol blend: engine performance and emissions. Fuel 2010;89(2):287–93.

[5] Zhang Z, Li G, Ouyang L, Pan Z, You F, Gao X. Experimental determination of laminar burning velocities and Markstein lengths for 75% hydrous-ethanol, hydrogen and air gaseous mixtures. Int J Hydrogen Energy 2011;36(20):13194–206.

[6] Park C, Choi Y, Kim C, Oh S, Lim G, Moriyoshi Y. Performance and exhaust emission characteristics of a spark ignition engine using ethanol and ethanol-reformed gas. Fuel 2010;89(8):2118–25.

[7] Shapouri H, Duffield JA, Wang M. The energy balance of corn ethanol revisited. Trans ASAE 2003;46(4):959–68.

[8] Macka JH, Aceves SM, Dibblea RW. Demonstrating direct use of wet ethanol in a homogeneous charge compression ignition (HCCI) engine. Energy 2009;34(6):782–7.

[9] Martinez-Frias J, Aceves SM, Flowers DL. Improving ethanol life cycle energy efficiency by direct utilization of wet ethanol in HCCI engines. J Energy Resour Technol ASME 2007;129(4):332–7.

[10] Bromberg L, Blumberg P. Estimates of DI hydrous ethanol utilization for knock avoidance and comparison to a measured and simulated DI E85 baseline. MIT Plasma Science & Fusion Center report PSFC/JA-09-33. http://www.psfc.mit.edu/library1/catalog/reports/2000/09ja/09ja033/09ja033_full.pdf; 2009.

[11] Cordon D, Clarke E. Catalytic igniter to support combustion of ethanol-water/air mixtures in internal combustion engines. SAE technical paper 2002-01-2863 2002.

[12] Haryanto A, Fernando S, Murali N, Adhikari S. Current status of hydrogen production techniques by steam reforming of ethanol: a review. Energy Fuels 2005;19(5):2098–106.

[13] Maeda T, Shinoki T, Funaki J, Hirata K. Hydrogen production by bio-fuel steam reforming at low-reaction temperature. In: ASME 2011 power conference collocated with JSME ICOPE 2011 (POWER2011); July 12–14, 2011. Denver, Colorado, USA.

[14] Sun J, Qiu XP, Wu F, Zhu WT. $H_2$ from steam reforming of ethanol at low temperature over $Ni/Y_2O_3$, $Ni/La_2O_3$ and $Ni/Al_2O_3$ catalysts for fuel-cell application. Int J Hydrogen Energy 2005;30(4):437–45.

[15] Hu YP, Li G, Yang Y, Gao X, Lu Z. Hydrogen generation from hydro-ethanol reforming by DBD-plasma. Int J Hydrogen Energy 2012;37(1):1044–7.

[16] Li G, You F, Gao X. Research on the application of hydrated alcohol for engine. J Wuhan Univ Technol-Transport Sci Eng 2008;32(6):994–7. [In Chinese].

[17] Dong J, Li G, Zhou Y, Zheng L. Impact of reformed ethanol on the volumetric efficiency in I.C. engines. SAE Int J Fuels Lubricants 2010;3(2):38–46.

[18] Bromberg L, Cohn DR. Heavy duty vehicles using clean, high efficiency alcohol engines. MIT Plasma Science & Fusion Center report PSFC/JA-10-43. http://www.psfc.mit.edu/library1/catalog/reports/2010/10ja/10ja043/10ja043_full.pdf; 2010.

[19] Li G, Zhang Z, Liang J, Dong F, Li Y, Gao X. Effects of hydrogen addition on the premixed laminar-flames of ethanol-air gaseous mixtures: an experimental study. Int J Hydrogen Energy 2012;37(5):4490–501.

[20] Ma F, Wang Y. Study on the extension of lean operation limit through hydrogen enrichment in a natural gas spark-ignition engine. Int J Hydrogen Energy 2008;33(4):1416–24.

[21] Al-Baghdadi MARS. Performance study of a four-stroke spark ignition engine working with both of hydrogen and ethyl alcohol as supplementary fuel. Int J Hydrogen Energy 2000;25(10):1005–9.

[22] Karim GA. Hydrogen as a spark ignition engine fuel. Int J Hydrogen Energy 2003;28(5):569–77.

[23] Wang S, Ji C, Zhang B. Effect of hydrogen addition on combustion and emissions performance of a spark-ignited ethanol engine at idle and stoichiometric conditions. Int J Hydrogen Energy 2010;35(17):9205–13.

[24] Wang J, Huang Z, Tang C, Zheng J. Effect of hydrogen addition on early flame growth of lean burn natural gas-air mixtures. Int J Hydrogen Energy 2010;35(13):7246–52.

[25] Yousufuddin S, Masood M. Effect of ignition timing and compression ratio on the performance of a hydrogen-ethanol fuelled engine. Int J Hydrogen Energy 2009;34(16):6945–50.

[26] Horng RF, Wen CS, Liauh CT, Chao Y, Huang CT. Driving characteristics of a motorcycle fuelled with hydrogen-rich gas produced by an onboard plasma reformer. Int J Hydrogen Energy 2008;33(24):7619–29.

[27] Bromberg L, Cohn DR, Rabinovich A, Surma JE, Virden J. Compact plasmatron-boosted hydrogen generation technology for vehicular applications. Int J Hydrogen Energy 1999;24(4):341–50.

[28] Bromberg L, Cohn DR, Rabinovich A, Heywood J. Emissions reductions using hydrogen from plasmatron fuel converters. Int J Hydrogen Energy 2001;26(10):1115–21.

[29] Kirwan JE, Quader AA, Grieve MJ. Advanced engine management using on-board gasoline partial oxidation reforming for meeting super-ULEV (SULEV) emissions standards. SAE technical paper 1999-01-2927 1999.

[30] Jamal Y, Wyszynski ML. On-board generation of hydrogen-rich gaseous fuels—a review. Int J Hydrogen Energy 1994;19(7):557–72.

[31] Tsolakis A, Torbati R, Megaritis A, Abu-Jrai A. Low-load dual-fuel compression ignition (CI) engine operation with an on-board reformer and a diesel oxidation catalyst: effects on engine performance and emissions. Energy Fuels 2010;24(1):302–8.

[32] Tsolakis A, Megaritis A. Partially premixed charge compression ignition engine with on-board $H_2$ production by exhaust gas fuel reforming of diesel and biodiesel. Int J Hydrogen Energy 2005;30(7):731–45.

[33] Hoffmann W, Wong VW, Cheng WK, Morgenstern DA. A new approach to ethanol utilization: high efficiency and low $NO_x$ in an engine operating on simulated reformed ethanol. SAE technical paper 2008-01-2415 2008.

[34] Morgenstern DA, Wheeler JC, Stein RA. High efficiency, low feedgas $NO_x$, and improved cold start enabled by low-temperature ethanol reforming. SAE Int J Engines 2010;3(1):529–45.

[35] Wheeler JC, Stein RA, Morgenstern DA, Sall ED, Taylor JW. Low-temperature ethanol reforming: a multi-cylinder engine demonstration. SAE technical paper 2011-01-0142 2011.

[36] Roh HS, Wang Y, King DL, Platon A, Chin YH. Low temperature and $H_2$ selective catalysts for ethanol steam reforming. Catal Lett 2006;108(1–2):15–9.

[37] Tartakovsky L, Mosyak A, Zvirin Y. Energy analysis of ethanol steam reforming for hybrid electric vehicle. Int J Energy Res 2013;37(3):259–67.

[38] Ji C, Dai X, Ju B, Wang S, Zhang B, Liang C, et al. Improving the performance of a spark-ignited gasoline engine with the addition of syngas produced by onboard ethanol steaming reforming. Int J Hydrogen Energy 2012;37(9):7860–8.

[39] Cavallaro S, Freni S. Ethanol steam reforming in a molten carbonate fuel cell. A preliminary kinetic investigation. Int J Hydrogen Energy 1996;21(6):465–9.
[40] Liguras DK, Kondarides DI, Verykios XE. Production of hydrogen for fuel cells by steam reforming of ethanol over supported noble metal catalysts. Appl Catal B Environ 2003;43(4):345–54.
[41] Salge JR, Deluga GA, Schmidt LD. Catalytic partial oxidation of ethanol over noble metal catalysts. J Catal 2005;235(1):69–78.
[42] Cavallaro S, Chiodo V, Freni S, Mondello N, Frusteri F. Performance of $Rh/Al_2O_3$ catalyst in the steam reforming of ethanol: $H_2$ production for MCFC. Appl Catal A Gen 2003;249(1):119–28.
[43] Vaidya PD, Rodrigues AE. Insight into steam reforming of ethanol to produce hydrogen for fuel cells. Chem Eng J 2006;117(1):39–49.
[44] You F, Hu Y, Li G, Gao X. Hydrogen generation from plasmatron reforming ethanol. J Wuhan Univ Technol 2006;28(Suppl. 1):64–8. [The 7th Chinese hydrogen energy conference].
[45] You F, Li G, Gao X. Study on reformed ethanol engine. In: Goswami DY, Zhao Y, editors. Solar 2007 world congress of the international-solar-energy-society: proceedings of ISES world congress 2007. Solar energy and human settlement, vols. I–V. Beijing, China. Berlin: Springer; 2009. p. 2418–21. 2007 Sep 18–21.
[46] Heywood JB. Internal combustion engine fundamentals. New York: McGraw-Hill; 1988.
[47] Ayastuy JL, Gutiérrez-Ortiz MA, González-Marcos JA, Aranzabal A, González-Velasco JR. Kinetics of the low-temperature WGS reaction over a $CuO/ZnO/Al_2O_3$ catalyst. Ind Eng Chem Res 2005;44(1):41–50.
[48] Divisek J, Oetjen HF, Peinecke V, Schmidt VM, Stimming U. Components for PEM fuel cell systems using hydrogen and CO containing fuels. Electrochim Acta 1998;43(24):3811–5.